Electron and Oxygen Transfer in Polyoxometalate, H 5 PV 2 Mo 10 O 40 , Catalyzed Oxidation of Aromatic and Alkyl Aromatic Compounds: Evidence for Aerobic Mars–van Krevelen-Type Rea...

ARTICLE *in* JOURNAL OF THE AMERICAN CHEMICAL SOCIETY · OCTOBER 2001

Impact Factor: 12.11 · DOI: 10.1021/ja004163z · Source: PubMed

Electron and Oxygen Transfer in Polyoxometalate, $H_5PV_2Mo_{10}O_{40}$, Catalyzed Oxidation of Aromatic and Alkyl Aromatic Compounds: Evidence for Aerobic Mars−van Krevelen-Type Reactions in the Liquid Homogeneous Phase

Alexander M. Khenkin,[†] Lev Weiner,[‡] Yan Wang,[§] and Ronny Neumann*,[†]

Contribution from the Department of Organic Chemistry, Weizmann Institute of Science, Rehovot, 76100 Israel, Chemical Services Division, Weizmann Institute of Science, Rehovot, 76100 Israel, and Casali Institute of Applied Chemistry, The Hebrew University of Jerusalem, Jerusalem, Israel, 91904

Received December 4, 2000

Abstract: The mechanism of aerobic oxidation of aromatic and alkyl aromatic compounds using anthracene and xanthene, respectively, as a model compound was investigated using a phosphovanadomolybdate polyoxometalate, $H_5PV_2Mo_{10}O_{40}$, as catalyst under mild, liquid-phase conditions. The polyoxometalate is a soluble analogue of insoluble mixed-metal oxides often used for high-temperature gas-phase heterogeneous oxidation which proceed by a Mars−van Krevelen mechanism. The general purpose of the present investigation was to prove that a Mars−van Krevelen mechanism is possible also in liquid-phase, homogeneous oxidation reactions. First, the oxygen transfer from $H_5PV_2Mo_{10}O_{40}$ to the hydrocarbons was studied using various techniques to show that commonly observed liquid-phase oxidation mechanisms, autoxidation, and oxidative nucleophilic substitution were not occurring in this case. Techniques used included (a) use of ^{18}O-labeled molecular oxygen, polyoxometalate, and water; (b) carrying out reactions under anaerobic conditions; (c) performing the reaction with an alternative nucleophile (acetate) or under anhydrous conditions; and (d) determination of the reaction stoichiometry. All of the experiments pointed against autoxidation and oxidative nucleophilic substitution and toward a Mars−van Krevelen mechanism. Second, the mode of activation of the hydrocarbon was determined to be by electron transfer, as opposed to hydrogen atom transfer from the hydrocarbon to the polyoxometalate. Kinetic studies showed that an outer-sphere electron transfer was probable with formation of a donor−acceptor complex. Further studies enabled the isolation and observation of intermediates by ESR and NMR spectroscopy. For anthracene, the immediate result of electron transfer, that is formation of an anthracene radical cation and reduced polyoxometalate, was observed by ESR spectroscopy. The ESR spectrum, together with kinetics experiments, including kinetic isotope experiments and ^1H NMR, support a Mars−van Krevelen mechanism in which the rate-determining step is the oxygen-transfer reaction between the polyoxometalate and the intermediate radical cation. Anthraquinone is the only observable reaction product. For xanthene, the radical cation could not be observed. Instead, the initial radical cation undergoes fast additional proton and electron transfer (or hydrogen atom transfer) to yield a stable benzylic cation observable by ^1H NMR. Again, kinetics experiments support the notion of an oxygen-transfer rate-determining step between the xanthenyl cation and the polyoxometalate, with formation of xanthen-9-one as the only product. Schemes summarizing the proposed reaction mechanisms are presented.

Introduction

In classic terms, homogeneous catalysis may be defined as a reaction in a liquid phase whereby a dissolved compound of well-defined molecular structure and property is used as a catalyst. Heterogeneous catalysis on the other hand usually occurs at a solid−gas or solid−liquid interface. The solid catalyst is often or usually ill-defined from the point of view of molecular structure. In the area of catalytic oxidation of hydrocarbons using molecular oxygen as oxidant, homogeneous and heterogeneous catalysis often also differ entirely as to the mechanism of oxidation and the mode of activation of molecular oxygen. Typically, in classic homogeneous liquid-phase aerobic oxidation, molecular oxygen reacts via the well-established metal-catalyzed free radical autoxidation pathways.[1] Additional possibilities include activation of molecular oxygen through formation of singlet oxygen;[2] use of oxygen to reoxidize redox active metals, as in Wacker-type reactions;[3] or activation in the presence of reducing agents, as is typical for monooxygenase enzymes and their mimetic counterparts.[4] There are also a few examples of activation of molecular oxygen by splitting of the oxygen−oxygen bond in the absence of a reducing agent.[5]

[†] Department of Organic Chemistry, Weizmann Institute of Science.
[‡] Chemical Services Division, Weizmann Institute of Science.
[§] The Hebrew University of Jerusalem.

(1) (a) Emanuel, N. M.; Denisov, E. T.; Maizus, Z. K. *Liquid Phase Oxidation of Hydrocarbons*; Plenum: New York, 1967. (b) Mayo, F. R. *Acc. Chem. Res.* **1968**, *1*, 193. (c) Howard, J. A. In *Free Radicals*; Kochi, J. K., Ed.; Wiley: New York, 1973; Vol. 2, p 3. (d) Betts, J. *Q. Rev. Chem. Soc.* **1971**, *25*, 265.

(2) Wasserman, H. H.; Murray, R. W. *Singlet Oxygen*; Academic Press: New York, 1978.

(3) (a) Jira, R.; Freiesleben, W. *Organomet. React.* **1972**, *3*, 1. (b) Gates, B. C.; Katzer, J. R.; Schuit, G. A. *Chemistry of Catalytic Processes*; McGraw-Hill: New York, 1969.

10.1021/ja004163z CCC: $20.00
Published on Web 08/08/2001

Scheme 1

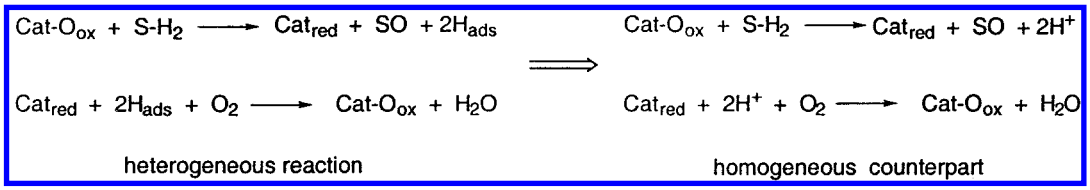

In gas phase, heterogeneous oxidation catalysis autoxidation pathways are significantly suppressed. Instead, especially with prevalent metal oxide catalysts, molecular oxygen activation often occurs via the well-known and established Mars−van Krevelen mechanism, Scheme 1.[6] This two-stage mechanism involves, first, C−H bond activation of a hydrocarbon, for example, by electron transfer and proton transfer from the hydrocarbon to the metal oxide, followed by lattice oxygen transfer from the oxide to yield the reaction product and the reduced catalyst. Second, there is reoxidation of the catalyst by molecular oxygen, coupled with formation of water. A typical example of an oxidation reaction of this kind is the oxidation of propylene to acrolein.[7]

Since the early 1970s, a significant body of catalysis research has dealt with the heterogenization of homogeneous catalysts.[8] The impetus of this research has been to combine the selectivity and milder conditions attainable by use of homogeneous catalysts with the catalyst-handling advantages inherent in heterogeneous catalysis. Typical approaches include attachment or support of homogeneous catalysts on insoluble matrixes[9] or use of biphasic liquid−liquid media,[10] whereby ideally, one phase contains the catalyst and the other contains the substrate and product. Interestingly, the idea of homogeneous analogues of heterogeneous catalysis is a considerably less developed area of research. However, in the field oxidation catalysis using transition metal oxides as catalysts, there are several conceivable advantages in the development of homogeneous analogues that can be identified. Thus, hydrocarbon activation and oxidation with molecular oxygen only via the Mars−van Krevelen mechanism would avoid the occurrence of radical chain, and generally nonselective, autoxidation reactions. In addition, heterogeneous oxidation reactions at high temperatures often are of reduced selectively as a result of over-oxidation to CO_x and are usually limited to simple and low-molecular-weight hydrocarbon molecules. Homogeneous analogues of such heterogeneous catalysis could, in principle, lead to viable, selective lower temperature aerobic oxidation of many hydrocarbons.

Because insoluble and often nonstoichiometric mixed metal oxides catalyze heterogeneous gas-phase oxidation reactions, a parallel homogeneous system would require the use of well-characterized, discrete, and soluble (mixed) metal oxides. Anionic polyoxometalates[11] are such compounds and, therefore, are attractive candidates for Mars−van Krevelen-type reactions in a homogeneous liquid phase. In this context, polyoxometalates have over the past decade or so attracted attention for their potential as oxidation catalysts[12] and in electron-transfer processes.[13] One approach to homogeneous catalysis by polyoxometalates has been to consider a lacunary polyoxometalate as an inorganic ligand to an active transition metal center. In the presence of a suitable oxidant, an active intermediate formed at the transition metal center leads to oxygenation of a substrate. Various oxidants or oxygen donors such as iodosobenzene,[14] *N*-oxides,[15] periodate,[16] ozone,[17] *tert*-butylhydroperoxide,[18] molecular oxygen[5c,d,19] and hydrogen peroxide,[20] have been shown to be effective for alkene and alkane oxidation. Another catalytic use of polyoxometalates in the liquid phase, using almost exclusively phosphovanadomolybdates, $PV_xMo_{12-x}O_{40}^{(3+x)-}$ ($x = 0, 1, 2$) (Figure 1), has been for oxidative dehydrogenation. Oxidative dehydrogenation of cyclic dienes, such as dihydroanthracene and α-terpinene,[21] alcohols and amines,[22] and

(4) (a) Ortiz de Montanello, P. *Cytochrome P-450*; Marcel Dekker: New York, 1986. (b) Sheldon, R. A. *Metalloporphyrins in Catalytic Oxidations*; Marcel Dekker: New York, 1994. (c) Montanari, F.; Casella, L. *Metalloporphyrin Catalyzed Oxidations*; Kluwer: Dordrecht, 1994. (d) Meunier, B. *Chem. Rev.* **1992**, *92*, 1411.

(5) (a) Groves, J. T.; Quinn, R. *J. Am. Chem. Soc.* **1985**, *107*, 5790. (b) Groves, J. T.; Ahn, K. H. *Inorg. Chem.* **1987**, *26*, 3831. (c) Neumann, R.; Dahan, M. *Nature* **1997**, *388*, 353. (d) Neumann, R.; Dahan, M. *J. Am. Chem. Soc.* **1998**, *120*, 11969.

(6) (a) Mars, P.; van Krevelen D. W. *Chem. Eng. Sci.* **1954**, *3*, 41. (b) Satterfield, C. N. *Heterogeneous Catalysis in Practice*; McGraw-Hill: New York, 1980.

(7) Burrington, J. D.; Kartisek, C. T.; Grasselli R. K. *J. Catal.* **1983**, *81*, 489.

(8) Cornils, B.; Herrmann, W. A. *Applied Homogeneous Catalysis with Organometallic Compounds*; VCH: Weinheim, 1996; Chapter 3.

(9) (a) Hartley, F. R. *Supported Metal Complexes*; Reidal: Dordrecht, 1985. (b) Sheldon, R. A. *Curr. Opin. Solid State Mater. Sci.* **1996**, *1*, 101. (c) Knops-Gerrits, P. P.; Vos, D. E.; Thibault-Starzyk, F.; Jacobs, P. A. *Nature* **1994**, *369*, 543. (d) Parton, R. F.; Vankelecom, I. F. J.; Casselman, M. J. A.; Bezoukhanova, C. P.; Uytterhoeven, J. B.; Jacobs, P. A. *Nature* **1994**, *370*, 541. (e) Vankelecom, I. F. J.; Tas, D.; Parton, R. F.; Van de Vyver, V.; Jacobs, P. A. *Angew. Chem., Int. Ed. Engl.* **1996**, *35*, 1346. (f) Rony, P. E. *J. Mol. Catal.* **1975**, *1*, 13. (g) Davis, M. E. *Chemtech* **1992**, 498.

(10) (a) Cornils, B.; Wiebus, E. *Chemtech* **1995**, 33. (b) Chaudhari, R. V.; Bhanage, B. M.; Deshpande, R. M.; Delmas, H. *Nature* **1995**, *373*, 501. (c) Chaudhari, R. V.; Bhattachyna, A.; Bhanage, B. M. *Catal. Today* **1995**, *24*, 123. (d) Horvath, I. T.; Rabai, J. *Science* **1994**, *266*, 72.

(11) Pope, M. T. *Heteropoly and Isopoly Oxometalates*; Springer: Berlin, 1983.

(12) (a) Mizuno, N.; Misono, M. *Chem. Rev.* **1998**, *98*, 199. (b) Okuhara, T.; Mizuno, N.; Misono, M. *Adv. Catal.* **1996**, *41*, 113. (c) Hill, C. L.; Duncan, D. C.; Harrup, M. K. *Comments Inorg. Chem.* **1993**, *14*, 367. (d) Hill, C. L.; Prosser-McCartha, C. M. *Coord. Chem. Rev.* **1995**, *143*, 407. (e) Neumann, R. *Prog. Inorg. Chem.* **1998**, *47*, 317. (f) Kozhevnikov, I. V. *Chem. Rev.* **1998**, *98*, 171. (g) Kozhevnikov, I. V. *Catal. Rev. Sci. Eng.* **1995**, *37*, 311.

(13) Weinstock, I. A. *Chem. Rev.* **1998**, *98*, 113.

(14) (a) Hill, C. L.; Brown, R. B. *J. Am. Chem. Soc.* **1986**, *108*, 536. (b) Mansuy, D.; Bartoli, J.-F.; Battioni, P.; Lyon, D. K.; Finke, R. G. *J. Am. Chem. Soc.* **1991**, *113*, 7222. (c) Weiner, H.; Hayashi, Y.; Finke, R. G. *Inorg. Chem.* **1999**, *38*, 2579.

(15) Zhang, X.; Sasaki, K.; Hill, C. L. *J. Am. Chem. Soc.* **1996**, *118*, 4809.

(16) (a) Neumann, R.; Abu-Gnim, C. *J. Chem. Soc., Chem. Commun.* **1989**, 1324. (b) Neumann, R.; Abu-Gnim, C. *J. Am. Chem. Soc.* **1990**, *112*, 6025. (c) Steckhan, E.; Kandzia, C. *Synlett* **1992**, 139. (d) Bressan, M.; Morvillo, A.; Romanello, G. *J. Mol. Catal.* **1992**, *77*, 283.

(17) Neumann, R.; Khenkin, A. M. *Chem. Commun.* **1998**, 1967.

(18) (a) Faraj, M.; Hill, C. L. *J. Chem. Soc., Chem. Commun.* **1987**, 1487. (b) Neumann, R.; Khenkin, A. M. *Inorg. Chem.* **1995**, *34*, 5753.

(19) (a) Lyons, J. E.; Ellis, P. E.; Durante, V. A. *Stud. Surf. Sci. Catal.* **1991**, *67*, 99. (b) Mizuno, N.; Hirose, T.; Tateishi, M.; Iwamoto, M. *J. Mol. Catal.* **1994**, *88*, L125. (c) Mizuno, N.; Tateishi, M.; Hirose, T.; Iwamoto, M. *Chem. Lett.* **1993**, 2137. (e) Katsoulis, D. E.; Pope, M. T. *J. Chem. Soc., Dalton Trans.* **1989**, 1483. (f) Neumann, R.; Dahan, M. *J. Chem. Soc., Chem. Commun.* **1995**, 171. (g) Neumann, R.; Dahan, M. *Polyhedron* **1998**, *17*, 3557. (h) Weiner, H.; Finke, R. G. *J. Am. Chem. Soc.* **1999**, *121*, 9831. (i) Mizuno, N.; Hirose, T.; Tateishi, M.; Iwamoto, M. *Chem. Lett.* **1993**, 1839. (j) Mizuno, N.; Tateishi, M.; Hirose, T.; Iwamoto, M. *Chem. Lett.* **1993**, 1985. (k) Khenkin, A. M.; Rosenberger, A.; Neumann, R. *J. Catal.* **1999**, *182*, 82. (l) Neumann, R.; Khenkin, A. M.; Dahan, M. *Angew. Chem., Int. Eng. Ed.* **1995**, *34*, 1587. (m) Hayashi, T.; Kishida, A.; Mizuno, N. *Chem. Commun.* **2000**, 381. (n) Khenkin, A. M.; Neumann, R. *Inorg. Chem.* **2000**, *39*, 3455.

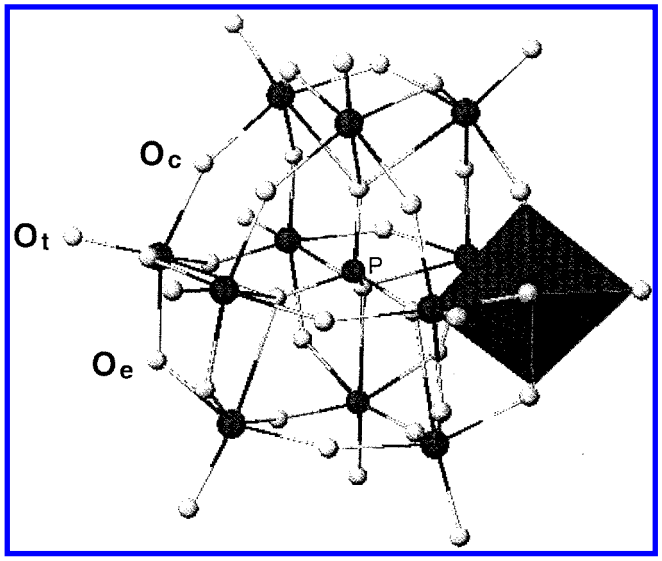

Figure 1. Ball-and-stick representation of the $PV_2Mo_{10}O_{40}^{5-}$ polyoxometalate highlighting one octahedral vanadium (molybdenum) position and noting the different types of oxygen atoms.

Scheme 2

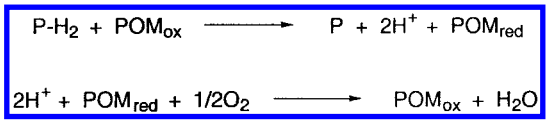

oxidation of phenols,[23] has been studied. In these cases, the substrates are oxydehydrogenated (electron and proton transfer from the substrate, $P-H_2$, to the polyoxometalate) but not oxygenated (oxygen transfer from the metal oxide) (Scheme 2).

In general, oxygen transfer through implementation of the Mars−van-Krevelen-type mechanism using molecular oxygen as the terminal oxidant[24] has until recently not been reported in liquid-phase homogeneous oxidation catalysis. In this connection, we have just recently published a preliminary communication describing such a catalytic process.[25] Here, we now present our more complete studies of our finding that vanadium containing polyoxometalates of the Keggin structure, $PV_2Mo_{10}O_{40}^{5-}$ (Figure 1), can activate C−H bonds in aromatic and alkyl aromatic compounds and oxygenate such substrates by a Mars−van Krevelen-type mechanism. We will also show and discuss the evidence for the activation of the hydrocarbon substrate by electron transfer, including observation of reaction intermediates, and present some insight on the oxygen-transfer step from the polyoxometalate to the activated hydrocarbon.

Results and Discussion

Oxygen Transfer from $H_5PV_2Mo_{10}O_{40}$ to Aromatic and Alkyl Aromatic Hydrocarbons. To investigate the oxidation of aromatic and alkyl aromatic compounds, relatively reactive anthracene and xanthene, respectively, were used as model substrates under aerobic, 1 atm pure O_2, conditions using the $H_5PV_2Mo_{10}O_{40}$ compound as catalyst. Thus, both anthracene and xanthene (60 mM) and a Keggin-type polyoxometalate, $H_5PV_2Mo_{10}O_{40}$ (1 mM), in acetonitrile were reacted under 1 atm molecular oxygen at 60 °C for 18 h. Analysis of the reaction mixture showed highly selective oxidation (>99%) of anthracene to anthraquinone and xanthene to xanthen-9-one at conversions of 92% and 96%, respectively. The polyoxometalate is stable under the reaction conditions; the ^{31}P NMR and IR are unchanged after the reaction. As indicated in the Introduction, a Mars−van Krevelen-type oxidation, Scheme 1, implies an oxygen transfer from the catalyst to an activated hydrocarbon intermediate. On the other hand, the well-accepted mechanism(s)[1,26] for oxidation of alkyl aromatic compounds in the liquid phase, Scheme 3, requires initiation of the reaction by the formation of a radical intermediate either by direct hydrogen atom abstraction (pathway a) or by electron transfer followed by deprotonation (pathway b). The following formation of the peroxo intermediate is very fast, in fact, diffusion-controlled. The peroxo intermediate can increase the radical chain length and, therefore, autocatalyze the reaction via formation of more alkyl radical species. At secondary alkyl aromatic positions, both alcohols and ketones are the major reaction products.

The liklihood of formation of radical intermediates in aromatic compounds without alkyl side chains is smaller as a result of the stronger C−H bonds. Thus, an additional pathway is possible via electron-transfer oxidation of the substrate coupled with nucleophilic attack[25,27] (Scheme 4).

An initially formed radical cation can react with a nucleophile, resulting in oxidative nucleophilic substitution. Using water and anthracene as the substrates, the tautomer of 9-hydroxyanthracene anthrone is formed. Under aerobic conditions, water is generated in a separate catalyst reoxidation step in a process similar to the one outlined in Scheme 2. Further reaction at the benzylic carbon of anthrone will yield anthraquinone. An alkyl aromatic substrate may also be oxygenated via an oxidative nucleophilic substitution. Here, initial electron transfer followed by further proton and electron transfer or hydrogen transfer will yield a benzylic cation. The latter would react with a nucleophile; thus, the oxidation of xanthene would yield xanthen-9-ol (Scheme 5).

According to the autoxidation pathway, Scheme 3, upon oxidation of hydrocarbons the only source of the oxygen atoms in the products is from atmospheric molecular oxygen; therefore, the oxidation of anthracene and xanthene was carried out using high-purity (96.1%) $^{18}O_2$. The isotope enrichment of anthraquinone and xanthen-9-one as a function of the turnover number is given in Figure 2. From the figure, one may observe that after one turnover, no ^{18}O was observed in the organic products; however, as the reaction continued, the ^{18}O isotope enrichment increased as a function of the number of turnovers. This

(20) (a) Khenkin, A. M.; Hill, C. L. *Mendeleev Commun.* **1993**, 140. (b) Neumann, R.; Gara, M. *J. Am. Chem. Soc.* **1994**, *116*, 5509. (c) Neumann, R.; Gara, M. *J. Am. Chem. Soc.* **1995**, *117*, 5066 (d) Neumann, R.; Khenkin, A. M. *J. Mol. Catal.* **1996**, *114*, 169. (e) Neumann, R.; Juwiler, D. *Tetrahedron* **1996**, *47*, 8781. (f) Neumann, R.; Khenkin, A. M.; Juwiler, D.; Miller, H.; Gara, M. *J. Mol. Catal.* **1997**, *117*, 169. (g) Mizuno, N.; Nozaki, C.; Kiyoto, I.; Misono, M. *J. Am. Chem. Soc.* **1998**, *120*, 9267. (h) Zhang, Z.; Chen, Q.; Duncan, D. C.; Lachicotte, R. J.; Hill, C. L. *Inorg. Chem.* **1997**, *36*, 4381. (i) Zhang, X.; Chen, Q.; Duncan, D. C.; Campana, C. F.; Hill, C. L. *Inorg. Chem.* **1997**, *36*, 4208. (j) Mizuno, N.; Seki, Y.; Nishiyama, Y.; Kiyoto, I.; Misono, M. *J. Catal.* **1999**, *184*, 550. (k) Mizuno, N.; Nozaki, C.; Kiyoto, I.; Misono, M. *J. Catal.* **1999**, *182*, 285. (l) Ben-Daniel, R.; Khenkin, A. M.; Neumann, R. *Chem. Eur. J.* **2000**, *6*, 3722.

(21) (a) Neumann, R.; Lissel, M. *J. Org. Chem.* **1989**, *54*, 4607. (b) Neumann, R.; Levin, M. *J. Am. Chem. Soc.* **1992**, *114*, 7278.

(22) Neumann, R.; Levin, M. *J. Org. Chem.* **1991**, *56*, 5707.

(23) (a) Kholdeeva, O. A.; Golovin, A. V.; Maksimovskaya, R. A.; Kozhevnikov, I. V. *J. Mol. Catal.* **1992**, *75*, 235. (b) Lissel, M.; Jansen van de Wal, H.; Neumann, R. *Tetrahedron Lett.* **1992**, *33*, 1795.

(24) Oxygen transfer from stable polyoxometalates ($Cr^V=O$) has been described, but the latter is prepared with iodosobenzene. Khenkin, A. M.; Hill, C. L. *J. Am. Chem. Soc.* **1993**, *115*, 8178.

(25) Khenkin, A. M.; Neumann, R. *Angew. Chem., Int. Ed.* **2000**, *39*, 4088.

(26) Sheldon, R. A.; Kochi, J. K. *Metal Catalyzed Oxidation of Orgainic Compounds*; Academic Press: New York, 1981.

(27) (a) Taylor, E. C.; McKillop, A. *Acc. Chem. Res.* **1970**, *3*, 338. (b) Fukuzumi, S.; Nakanishi, I.; Tanaka, K. *J. Phys. Chem. A* **1999**, *103*, 11212.

Scheme 3

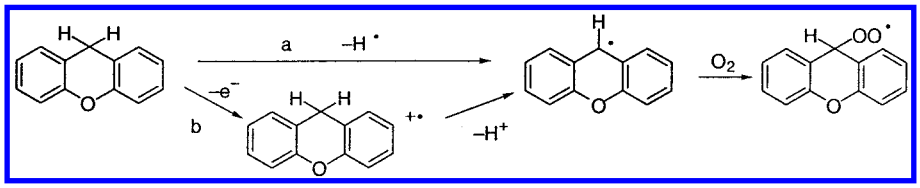

Scheme 4

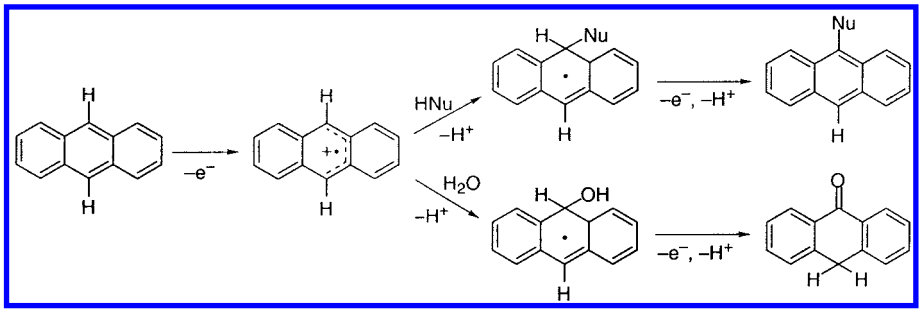

Scheme 5

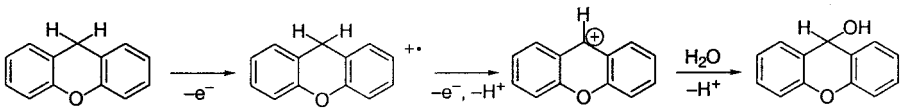

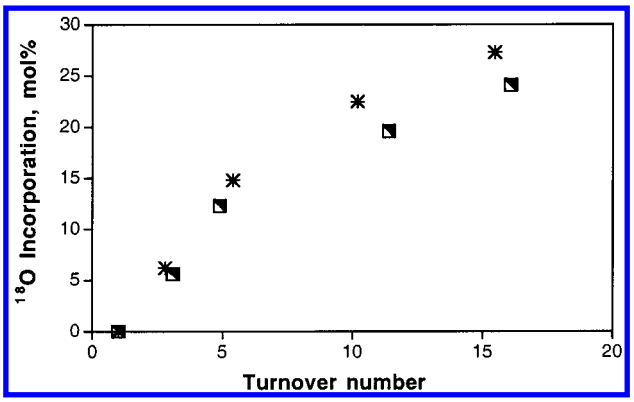

Figure 2. ^{18}O incorporation as a function of the turnover number. Reaction conditions: anthracene or xanthene (20 mM) and $H_5PV_2Mo_{10}O_{40}\cdot 34H_2O$ (1mM) in CH_3CN under 1 atm $^{18}O_2$ (96.1% purity) at 60 °C. The amount of ^{18}O in the product was determined by GC/MS. Asterisk (*), anthracene; ◥, xanthene.

experiment clearly indicates that the source of the ^{18}O in the products is not directly from the molecular oxygen. The results, however, do comply with a Mars−van Krevelen mechanism whereby the original catalyst contains only ^{16}O. As the reaction advances, the polyoxometalate is enriched with ^{18}O, and thus, the product is progressively labeled. In this context, it should be noted that there is no exchange of lattice oxygen of $H_5PV_2Mo_{10}O_{40}$ with labeled molecular oxygen in the absence of substrate, even after 2 weeks. Furthermore, after one turnover, the expected amount of $H_2{}^{18}O$ was observed (1 ± 0.2 μmol). ^{18}O incorporation in the polyoxometalate was also observed by the isotope shifts in the IR spectrum. The curves in Figure 2 tend to level off instead of continuing in a linear fashion. This is due to the fact that water does exchange oxygen atoms in the polyoxometalate framework, and $H_2{}^{16}O$ is already present at the beginning of the reaction (~50 mol water from hydrate and solvent/mol polyoxometalate). From separate measurements, the equilibration reaction (water−polyoxometalate) is relatively fast (within 30 min at 60 °C), as compared with the oxidation reaction. At low turnover number (1−5), the ^{18}O load in the polyoxometalate is low, and the excess $H_2{}^{16}O$ has little effect. As the reaction continues (TON 8−15), the excess $H_2{}^{16}O$ ($H_2{}^{16}O/H_2{}^{18}O = 5 \pm 1$) dilutes the ^{18}O load in the polyoxometalate, leading to the observed nonlinearity in Figure 2.

An additional test of a Mars−van Krevelen versus free radical mechanism can be carried out by performing the reaction under strictly anaerobic conditions. Thus, independent reactions of equimolar amounts of anthracene or xanthene and $H_5PV_2Mo_{10}O_{40}$ (1 mM in CD_3CN) were carried out at 60 °C for 24 h under argon in a NMR tube and yielded by ^{1}H NMR up to 48% anthraquinone and 71% xanthen-9-one, respectively. Because each polyoxometalate molecule can be formally considered a three-electron oxidant,[28] the maximum theoretical or possible conversions to anthraquinone and xanthen-9-one by a Mars−van Krevelen mechanism are 50% and 75%, respectively (Scheme 6).

Further support for showing that the source of oxygen in the oxidation product is the polyoxometalate rather than molecular oxygen can be found by carrying out similar independent anaerobic reactions of equimolar amounts (1 mM in CH_3CN) of anthracene or xanthene and $H_5PV_2Mo_{10}{}^{18}O_{40}$ (75% enrichment). GC/MS analysis of the products showed that the anthraquinone was 70% ^{18}O-labeled, whereas the xanthen-9-one was 72% ^{18}O-labeled. The reaction stoichiometries, molecular oxygen/anthracene and molecular oxygen/xanthene, must be 1.5/1 and 1/1 to support a Mars−van Krevelen mechanism. Indeed, O_2 consumption was measured using a gas buret in an aerobic reaction [anthracene or xanthene (60 mM), $H_5PV_2Mo_{10}O_{40}$ (1 mM) in acetonitrile, 1 atm O_2, 60 °C, 18 h]. The ratios were found to be 1.45 ± 0.2 equiv/reaction cycle for anthracene and 0.95 ± 0.3 equiv/reaction cycle for xanthene.

The results presented above quite conclusively go against the formulation of an autoxidation mechanism, Scheme 3, for the oxidation of either xanthene or anthracene. It is also worth

(28) One electron is transferred in the initial polyoxometalate−hydrocarbon interaction, and during the oxygen transfer, there is an additional reduction of the polyoxometalate.

Scheme 6

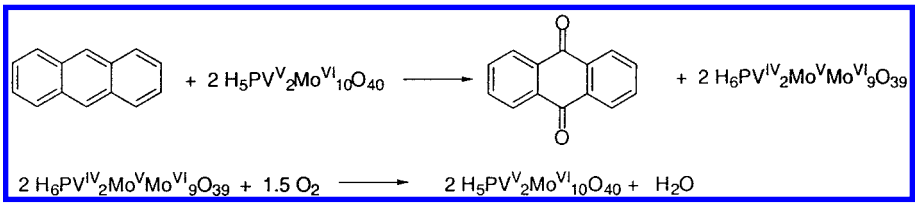

mentioning in this context that a compound, such as cyclohexene, that is highly sensitive to autoxidation does not react under the given reaction conditions. The results, however, do not all necessarily disprove an oxidative nucleophilic pathway (Schemes 4 and 5), whereby the reduced polyoxometalate is reoxidized, as indicated in Scheme 2. This possibility should be especially considered, because the $H_5PV_2Mo_{10}O_{40}$ catalyst was used as a hydrate, because dehydrated $H_5PV_2Mo_{10}O_{40}$ is insoluble in acetonitrile. In such a mechanistic scheme, the immediate source of oxygen in the product is water, which is continually replaced by molecular oxygen in the reoxidation process. The most obvious way to discount the oxidative nucleophilic pathway is to perform the reaction under anhydrous conditions. Therefore, the nonhydrated acetonitrile soluble quaternary ammonium salt $Q_5PV_2Mo_{10}O_{40}$ (Q = tetrabutylammonium) was used as catalyst in place of the hydrate of $H_5PV_2Mo_{10}O_{40}$. Unfortunately, the oxidation potential of polyoxometalates is significantly affected by the countercation and the acidity of the solvent. The nonprotic form of the catalyst has a significantly reduced oxidation potentia,[29] and in acetonitrile, no reduction of the polyoxometalate or hydrocarbon oxidation was observed. However, with anhydrous but somewhat acidic 1,1,1,3,3,3-hexafluoro-2-propanol as solvent, the oxidation of 20 mM anthracene or xanthene in the presence of 1 mM $Q_5PV_2Mo_{10}O_{40}$ (55 °C, 1 atm O_2, 16 h) was possible. Both anthraquinone, 20% yield, and xanthen-9-one, 33% yield, were observed as the only products. A second obvious experiment is to perform the reaction using isotopically enriched water in place of the usual hydrate, that is, $H_5PV_2Mo_{10}O_{40}$ in the presence of $H_2{}^{18}O$. As noted above, this experiment is complicated by the fact that there is relatively fast oxygen atom exchange between water and the terminal, edge-shared, and corner-shared oxygen atoms in the $H_5PV_2Mo_{10}O_{40}$ polyoxometalate. At 60 °C, one can estimate by the IR isotope shifts, a 30 ± 5% exchange within 15 min. Despite this limitation, reactions between equimolar amounts of anthracene or xanthene (1 mM) and $H_5PV_2Mo_{10}O_{40}$ (1 mM, dried), 500 mM $H_2{}^{16}O$, and 500 mM $H_2{}^{18}O$ (1/1 $H_2{}^{16}O/H_2{}^{18}O$) in dry acetonitrile at 60 °C under argon were carried out. The $^{16}O/^{18}O$ isotope ratios in the product were measured after 15 min (~3−5% conversion). The results showed $^{16}O/^{18}O$ isotope ratios of 4.2 for anthracene and 4.5 for xanthene versus the approximately 1/1 ratio that would have been expected if the oxygen atom in the product came from water rather than an oxygen atom of the polyoxometalate. A third experiment that pointed toward a Mars−van Krevelen mechanism and against an oxidative nucleophilic substitution was to perform the reaction in the presence of acetic acid as an alternative nucleophile instead of water. A nucleophilic attack by acetic acid would be expected to yield some of the known acetates[30] instead of only the observed quinone or ketone (Schemes 4 and 5). Reactions under the following conditions: anthracene or xanthene (20 mM), $H_5PV_2Mo_{10}O_{40}\cdot 34H_2O$, and acetic acid (160 mM) at 60 °C under 1 atm O_2 for 16 h, showed no formation of any acetylated hydrocarbons. Only anthraquinone and xanthen-9-one (90 and 94% conversion, respectively) were obtained. Together, the three experiments described disprove the possibility of an oxidative nucleophilic mechanism to account for the product of the formation of anthraquinone and xanthen-9-one. An additional point very worth noting in this context is that the oxidative nucleophilic mechanism first requires the formation of anthrone and xanthen-9-ol. These products were never observed (see also the ^{1}H NMR experiments discussed latter on).

Scheme 7

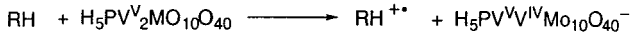

All of the experiments described above are consistent with a Mars−van Krevelen mechanism; the experiments described are inconsistent with autoxidation or oxidative nucleophilic substitution mechanisms.

Activation of Hydrocarbons with $H_5PV_2Mo_{10}O_{40}$. For oxidation catalysis to occur, the catalyst must first activate the hydrocarbon. One possible mode of activation is electron transfer from the hydrocarbon to the $H_5PV_2Mo_{10}O_{40}$ polyoxometalate to yield initially a radical cation of the hydrocarbon and a one-electron reduced $H_5PV_2Mo_{10}O_{40}$ (Scheme 7.)[31] Alternatively, hydrogen abstraction and formation of a caged radical species can be considered.[32]

The activation of the hydrocarbon was initially studied kinetically by mixing the hydrocarbons and polyoxometalate in solution under argon and following the appearance of a reduced blue species, $PV^VV^{IV}Mo_{10}O_{40}{}^{6-}$, at 750 nm in the visible spectrum. Kinetic profiles were obtained from the reaction of 1 μmol of $H_5PV_2Mo_{10}O_{40}$ and 20 μmol of hydrocarbon in 3 mL acetonitrile under argon at 60 °C and showed that the reactions were first-order in $H_5PV_2Mo_{10}O_{40}$ and pseudo-zero-order in the substrate, which was in excess. The interaction of $H_5PV_2Mo_{10}O_{40}$ with hydrocarbons having aromatic C−H bonds, such as anthracene, 2-methoxyanthracene, 2-chloroanthracene, anthracene-d_{10}, and phenanthrene, and hydrocarbons with benzylic C−H bonds, such as xanthene, 2-methylanthracene, fluorene, and diphenylmethane, was measured. The gas-phase ionization potential,[33] which was used as a measure of the oxidation potential of the hydrocarbon, showed a very good correlation ($r^2 = 0.93$) as a function of the rate constant (Figure 3). Because the nonbenzylic compounds have strong C−H bonds at the reactive position, ~105 kcal/mol, and the benzylic compounds have weaker C−H bonds at the reaction site, 80−85 kcal/mol, it is clear that there was no correlation of the rate as a function of the C−H bond strength. The results appear to support an electron-transfer reaction rather than a hydrogen atom transfer process for activation of the hydrocarbons by the polyoxometalate. For further support of this conclusion, the interaction of $H_5PV_2Mo_{10}O_{40}$ with 4-methyl-, 4-ethyl-, and 4-*i*-propylanisole was also investigated. The relative reactivity of

(29) (a) Carloni, P.; Eberson, L. *Acta Chem. Scand.* **1991**, *45*, 373. (b) Keita, B.; Bouaziz, D.; Nadjo, L. *J. Electrochem. Soc.* **1988**, *135*, 87.

(30) (a) Koshitani, J.; Hiramatsu, M.; Ueno, Y.; Yoshida, T. *Bull. Chem. Soc., Jpn.* **1978**, *51*, 3667. (b) Hanotier, J.; Hanotier-Bridoux, M.; de Radadzitzky, P. *J. Chem. Soc., Perkin Trans. 2* **1973**, 381.

(31) Shaik, S.; Shurki, A. *Angew. Chem., Int. Ed.* **1999**, *38*, 587.

(32) Mayer, J. M. *Acc. Chem. Res.* **1998**, *31*, 441.

(33) Taken from the NIST at http://webbook.nist.gov/chemistry

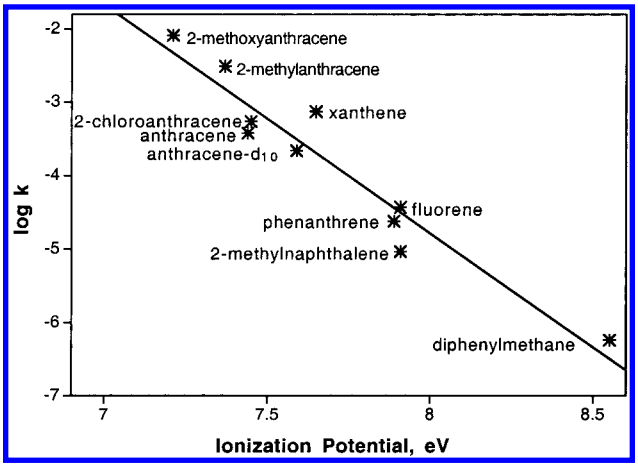

Figure 3. Reaction of $H_5PV_2Mo_{10}O_{40}$ with hydrocarbons as a function of the gas-phase ionization potential. The reduction of $H_5PV_2Mo_{10}O_{40}$ was followed by a diode array UV−vis spectrometer reading at 750 nm. Conditions: 1 μmol of $H_5PV_2Mo_{10}O_{40}$ and 20 μmol of hydrocarbon in 3 mL of acetonitrile under argon at 60 °C.

Table 1. Rate Constants for the Reduction of $H_5PV_2Mo_{10}O_{40}$ by 4-Alkylanisoles[a]

substrate	rate constant, sec^{-1}	relative rate
4-methylanisole	3.00×10^{-5}	0.12
4-ethylanisole	2.59×10^{-4}	1
4-*i*-propylanisole	4.51×10^{-5}	0.18

[a] Reaction conditions: 1 μmol of $H_5PV_2Mo_{10}O_{40}$ and 10 μmol of 4-alkylanisole in 3 mL of acetonitrile under argon at 60 °C.

the 4-alkylanisole compounds has also been used in the past as a test for electron transfer versus hydrogen atom transfer reactions.[34] For electron-transfer reactions, the relative rates are 2° > 1° > 3° or 2° > 3° > 1°, whereas for hydrogen atom transfer reactions, it is always found that 3° > 2° > 1°. Thus, reactions of 4-alkylanisole with $H_5PV_2Mo_{10}O_{40}$ were studied as above by reacting 1 μmol $H_5PV_2Mo_{10}O_{40}$ and 20 μmol substituted anisole in 3 mL acetonitrile under argon at 60 °C. From the kinetic profiles which also, as above, showed first-order behavior for the reduction of $H_5PV_2Mo_{10}O_{40}$, one can observe that the reaction is fastest for 4-ethylanisole > 4-*i*-propylanisole > 4-methylanisole (Table 1). From the results described above, which are also supported by examples to be found in the literature describing oxydehydrogenation of other substrates,[13] such as dienes[21b] and phenols,[23b] and photoactivated oxydehydrogenation,[35] it would certainly appear that the initial hydrocarbon−polyoxometalate reaction is an electron-transfer process.

To gain more insight into the electron-transfer process, in particular in order to distinguish between outer-sphere and inner-sphere-type reactions, the electron-transfer reaction of $H_5PV_2Mo_{10}O_{40}$ with three select hydrocarbons, anthracene, xanthene, and 4-ethylanisole, was measured as a function of temperature (Figure 4). The plot enables the computation of the activation parameters, and in Table 2 are summarized all of the thermodynamic data for the electron-transfer step between $H_5PV_2Mo_{10}O_{40}$ and the three substrates. The free energy of reaction, $\Delta G°$, was computed from $\Delta E°$ ($\Delta G° = 23.06\Delta E°$ kcal/mol) using an oxidation potential of 0.69 V for $H_5PV_2Mo_{10}O_{40}$ in acetonitrile, as measured by cyclic voltammetry. The free energy under prevailing reaction conditions was corrected by an

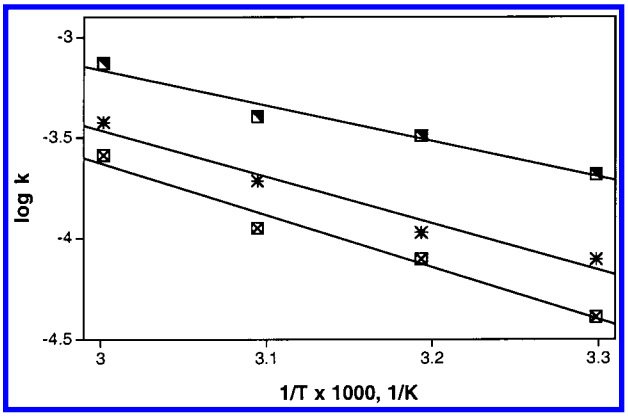

Figure 4. Reaction of $H_5PV_2Mo_{10}O_{40}$ with several hydrocarbons as a function of temperature. The reduction of $H_5PV_2Mo_{10}O_{40}$ was followed by a diode array UV−vis spectrometer reading at 750 nm. Conditions: 1 μmol of $H_5PV_2Mo_{10}O_{40}$ and 20 μmol of hydrocarbon in 3 mL of acetonitrile under argon at 30−60 °C. Asterisk (*), anthracene; ◥, xanthene; X in a box, 4-ethylanisole.

Table 2. Thermodynamic Data for the Electron-Transfer Step between $H_5PV_2Mo_{10}O_{40}$ and Hydrocarbons

compd	$\Delta H^‡$ kcal/mol	$\Delta S^‡$ cal/mol K	$\Delta G^‡$ kcal/mol	$E°$V vs SCE	$\Delta G°$ kcal/mol	$\Delta G°'$ kcal/mol
anthracene	9.4	−42.5	22.0	1.37[a]	15.7	7.9
xanthene	6.8	−48.5	21.3	1.49[b]	18.5	10.7
4-ethylanisole	10.6	−39.6	22.3	1.52[c]	19.1	11.4

electrostatic term[36] to give the corrected free energy value, $\Delta G°'$ (eq 1).

$$\Delta G°' = \Delta G° + \frac{331.2B}{r_{12}D}(Z_1 - Z_2 - 1) \quad \text{where} \quad B = 10^{-(21.9r_{12}\sqrt{\mu/DT})} \quad (1)$$

$B = 1$ assuming an ion strength, $\mu = 0$ and $Z_1 = -5$; $Z_2 = 0$; $D = 35$ (acetonitrile); $r_{12} = r_1 + r_2 = 5.6$ Å ($H_5PV_2Mo_{10}O_{40}$) + 1.7 Å (assuming side-on interaction between the polyoxometalate and the aromatic ring) = 7.3 Å.

In general, the free energy values, both $\Delta G°$ and $\Delta G°'$ versus $\Delta G^‡$ appear to support an outer-sphere electron transfer, as opposed to an inner-sphere process for activation of the hydrocarbon by $H_5PV_2Mo_{10}O_{40}$. However, as already pointed out by others, the kinetic analysis of the reaction of polyoxometalates with electron donors may be complicated by several phenomena.[13,37] These include effects of ionic strength, ion pairing between the polyoxometalate and any cations in the solution, and formation of stable complexes between the polyoxometalate and the electron donor (hydrocarbon). First, it should be noted that there is clear evidence for the formation of stable complexes after electron transfer, as indicated from the analysis of the ESR spectrum (see below) of the reaction between anthracene and $H_5PV_2Mo_{10}O_{40}$. Also relevant are further fast or possibly concurrent proton, electron, or atom transfers, as is indicated in the interpretation of the ^1H NMR spectrum (see below) of the reaction between xanthene and $H_5PV_2Mo_{10}O_{40}$. The probable existence of preassociation complexes between the polyoxometalate and the hydrocarbon substrates may be inferred from calculated reorganization energies. Assuming that there are no preassociation complexes, the Marcus equation, eq 2, yields computed reorganization

(34) Baciocchi, E.; D'Acunzo, F.; Galli, C.; Lanzalunga, O. *J. Chem. Soc., Perkin Trans. 2* **1996**, 133.
(35) Renneke, R. F.; Hill, C. L. *J. Am. Chem. Soc.* **1988**, *110*, 5461.
(36) Eberson, L. *Adv. Phys. Org. Chem.* **1982**, *18*, 79.
(37) Eberson, L. *New J. Chem.* **1992**, *16*, 151.

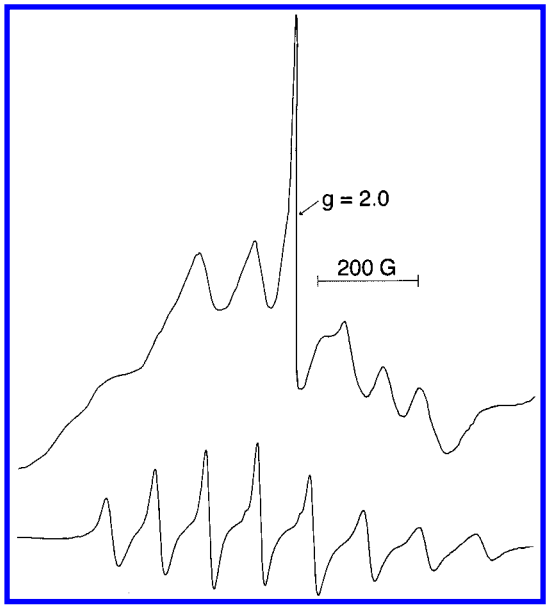

Figure 5. ESR spectrum of a solution of $Q_5PV_2Mo_{10}O_{40}$ and anthracene. Top: 4 mM $Q_5PV_2Mo_{10}O_{40}$ and 2 mM anthracene in 1,1,1,3,3,3-hexafluoro-2-propanol under argon were reacted for 20 min at 40 °C prior to the measurement of the ESR spectrum at room temperature. Bottom: 4 mM $H_5PV_2Mo_{10}O_{40}$ and 2 mM anthracene in acetonitrile under argon were reacted for 20 min at 40 °C prior to the measurement of the ESR spectrum at room temperature.

energies, λ, of 102, 94, and 96 kcal/mol for anthracene, xanthene, and 4-ethylanisole, respectively. These values are seemingly and illogically high. If, however, electron transfer is occurring within a stable preassociation complex, the Marcus equation should be modified by dropping the Coulombic work term, $W(r)$, and not applying the electrostatic correction to $\Delta G°$, leaving only a quadratic dependence of $\Delta G^{‡}$ on $\Delta G°$, eq 3. The reorganization energies, λ, which now may be calculated from this latter expression are 52, 40, and 43 kcal/mol for anthracene, xanthene and 4-ethylanisole, respectively. Thus, it would appear that there is preassociation between the polyoxometalate and the hydrocarbon substrate.

$$\Delta G^{‡} = W(r) + \frac{\lambda}{4}\left(1 + \frac{\Delta G°'}{\lambda}\right)^2 \quad (2)$$

$$\Delta G^{‡} = \frac{\lambda}{4}\left(1 + \frac{\Delta G°}{\lambda}\right)^2 \quad (3)$$

The isotope effect in the electron-transfer step was measured by comparing the rate of reduction of $H_5PV_2Mo_{10}O_{40}$ with nondeuterated and deuterated hydrocarbons. For anthracene/anthracene-d_{10} the ratio, $k_H/k_D = 1.7$ was measured. The source of this isotope effect appears from the linear relationship between the ionization potential and the rate observed in Figure 3 to be entirely due to the different ionization potentials of anthracene and anthracene-d_{10}, rather than to be due to any effect of hydrogen or proton disassociation during the electron-transfer step. A similar comparison between xanthene and xanthene-9-d_2 gave a ratio, $k_H/k_D = 2.3 \pm 0.08$. This higher k_H/k_D value for xanthene, as compared with anthracene, suggests a different explanation (see below), especially since only the benzylic carbon, but not the aromatic carbons, is deuterated. Only deuteration at the aromatic rings would most likely have an effect on the ionization potential. Unfortunately, ionization potentials were not available for xanthene-9-d_2; however, cyclic voltammetry measurements of xanthene and xanthene-9-d_2 gave

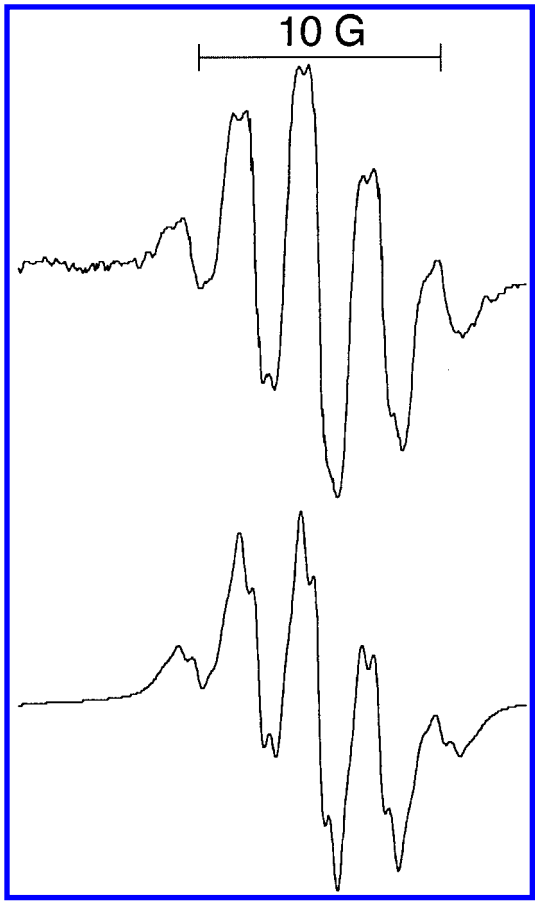

Figure 6. Expanded ESR spectrum of Figure 5 (top) at $g = 2.0027$ (top) and computer simulation of the radical cation species (bottom).

practically identical I−V curves and an $E° = 1.58$ V versus SCE. In the past, significantly higher isotope effects, $k_H/k_D = \sim 6$, have been observed in the electron transfer from alkyl aromatic substrates such as 4-methylanisole. In that case, the effect was ascribed to concurrent proton transfer during the electron-transfer step.[38]

Observation of Reaction Intermediates. From the experiments described above, one may conclude that the hydrocarbon is activated by electron transfer to the polyoxometalate, resulting in the formation of a radical cation and the mono-reduced $PV^{IV}V^{V}Mo_{10}O_{40}^{6-}$. We sought to observe this radical cation in situ. In the case of anthracene and in acetonitrile as solvent, the spectrum of the reduced paramagnetic polyoxometalate was observed; however, we were unable to observe a radical cation under these conditions. We turned to the use of 1,1,1,3,3,3-hexafluoro-2-propanol (HFIP) as solvent, since this solvent is known for its ability to stabilize radical cations.[39] Therefore, anthracene or xanthene and $Q_5PV_2Mo_{10}O_{40}$ in HFIP were reacted under argon. These conditions allowed for the observation (overlapped) of both the reduced polyoxometalate (Figure 5, top) and the anthracene radical cation (Figure 6). First, concerning the spectrum of the reduced paramagnetic $PV^{IV}V^{V}Mo_{10}O_{40}^{6-}$, one may observe that it is distinctly distorted compared to the spectrum of $PV^{IV}V^{V}Mo_{10}O_{40}^{6-}$ formed in acetonitrile (Figure 5, bottom), which does not involve associated radical cations or radical species.[19k] We attribute the distortion to the interaction of the polyoxometalate with the anthracene radical cation. Second, the spectrum of the species

(38) Eberson, L.; Wistrand, L.-G. *Acta Chem. Scand. B* **1980**, *34*, 349.
(39) Eberson, L.; Hartshorn, M. P.; Persson, O. *J. Chem. Soc., Perkin Trans. 2* **1995**, 1735.

at $g = 2.0027$ (Figure 6) is, indeed, indicative of the formation of an anthracene radical cation.[40] The spectrum consists of five split components in an integrated ratio of 1:4:6:4:1. Additional splitting of the quintet was also observed. Computer simulation of the experimental spectrum yielded the hyperfine splitting constants, $a_{1,4,5,8} = 3.4$ G, $a_{2,3,6,7} = 0.95$ G, and $a_{9,10} = \sim 0$. Comparison of these hyperfine splitting constants with those of a "pure" anthracene radical cation in which splitting constants of $a_{1,4,5,8} = 3.08$ G, $a_{2,3,6,7} = 1.39$ G, and $a_{9,10} = 6.60$ G were measured reveals that there is a good agreement for $a_{1,4,5,8}$ and $a_{2,3,6,7}$, but not for $a_{9,10}$. The disappearance of the hyperfine splitting associated with the 9,10 hydrogen atoms has also previously been observed.[41] For example, in trifluoracetic acid, a splitting constant of $a_{9,10} = 0.25$ G has been obtained and associated with hydrogen bonding between the hydrogen of anthracene at the 9(10) position and the trifluoroactetate. In this case, we believe that the loss of hyperfine splitting is due to the ion pairing between the polyoxometalate and the reactive position of the anthracene radical cation. Even though we observed a radical cation species in a medium that leads to product formation, it should also be shown that the electron-transfer step is on the reaction pathway to the anthraquinone product. Thus, after reacting anthracene and $Q_5PV_2Mo_{10}O_{40}$ for 30 min, quantification of the anthracene radical cation by double integration techniques shows ~20 mol % conversion. A separate UV−vis analysis of the degree of reduction of $Q_5PV_2Mo_{10}O_{40}$ indicated a similar 20% conversion. This correlation supports the idea that the radical cation of anthracene is an intermediate in the formation of anthraquinone. Although we were successful in observing the anthracene radical cation, in similar experiments with xanthene, only the spectrum of the reduced $PV^{IV}V^{V}Mo_{10}O_{40}^{6-}$ species was observed. The radical cation of xanthene was not observed by ESR spectrometry.

The reaction of anthracene or xanthene with $H_5PV_2Mo_{10}O_{40}$ in acetonitrile solutions was also followed by ^{1}H NMR spectroscopy. A reaction carried out in a NMR tube between anthracene (2 mM anthracene, 4 mM $H_5PV_2Mo_{10}O_{40}$ in CD_3CN under argon at 60 °C), showed only the clean formation of anthraquinone. No intermediate species or products such as anthrone were observed. A similar experiment with xanthene as substrate (2 mM xanthene, 4 mM $H_5PV_2Mo_{10}O_{40}$ in CD_3CN under argon at 60 °C) gave an entirely different result (Figure 7). In the NMR spectrum, there first appears after 20 min an intermediate species (Figure 7, bottom). As the reaction continues and after an additional 20 min, the formation of the product, xanthen-9-one (marked p in the middle spectrum) becomes apparent. The intermediate remains at an approximately constant concentration. The spectrum of the intermediate species appears to be very similar to the spectrum reported for a xanthenyl cation, which was measured in 98% D_2SO_4.[42] The assignment of the peaks in this context is 10.37 ppm (s, $1H_9$), 8.65 ppm (bs, $4H_{1\&3}$), 8.38 ppm (d, $2H_4$), and 8.10 ppm (t, $2H_2$). Notable also is the fact that xanthen-9-ol with ^{1}H NMR peaks at 7.48 ppm (d, 2H), 7.29 ppm (m, 2H) 7.10 ppm (m, 2H), 5.68 (d, 1H-benzylic) and 2.50 (d, 1H-hydroxyl) was not detected. From the ^{1}H NMR experiment for the case of xanthene, it would be reasonable to conclude that a proton and then additional electron transfer to yield a benzylic cation as an intermediate quickly follow the initial electron transfer. The logic behind this hypothesis stems from the fact that benzylic radical cations are extremely strong acids[43] and from calculations are ~10 orders magnitude stronger acids than aromatic radical cations.[43] The electron-donating oxygen heteroatom in xanthene stabilizes the benzylic cation. Interaction and stabilization of the benzylic cation and polyoxometalate anion by ion pairing or complex formation is certainly also very conceivable.

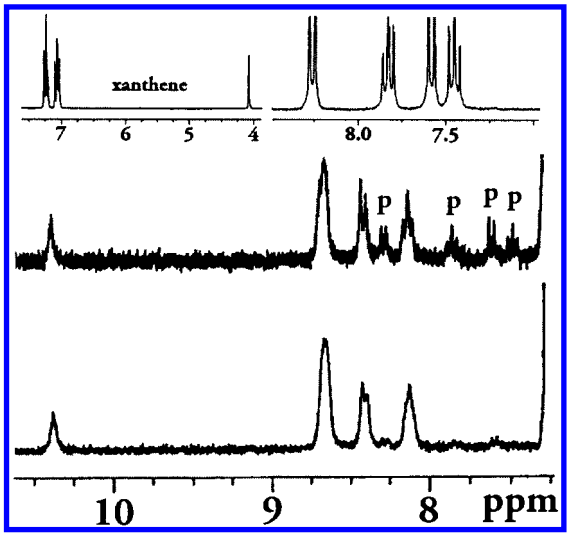

Figure 7. ^{1}H NMR spectra of the reaction between xanthene and $H_5PV_2Mo_{10}O_{40}$. Reaction conditions: 10 mM xanthene and 10 mM $H_5PV_2Mo_{10}O_{40}$ in 0.5 mL of CD_3CN under argon.

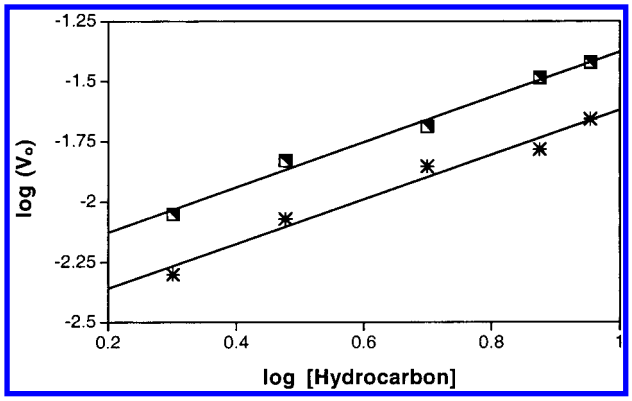

Figure 8. Rate of reaction as a function of hydrocarbon concentration. Reaction conditions: 2−9 mM substrate and 1 mM $H_5PV_2Mo_{10}O_{40}$ in 2 mL of acetonitrile, 1 atm O_2, 60 °C. Asterisk (*), anthracene; ◥, xanthene.

Reaction Kinetics in the Aerobic Oxidation. To shed more light on the reaction mechanism and to determine the rate-limiting step in the oxidation reaction, the kinetics of the aerobic oxidation of both xanthene and anthracene was studied. First, reaction order in each of the reaction components was determined by using the method of initial rates. Logarithmic van't Hoff plots, in which rate constants were obtained from series of reaction profiles, were used to find the reaction order in the hydrocarbon (2−9 mM) (Figure 8), polyoxometalate (0.25−2 mM) (Figure 9), and molecular oxygen (0.2−3 atm) (Figure 10). The reaction was found to be first-order in the hydrocarbon; the slopes in the van't Hoff plots were 0.93 ($r^2 = 0.98$) and 0.94 ($r^2 = 0.99$) for anthracene and xanthene, respectively. Similarly, the reaction was observed also to be first-order in $H_5PV_2Mo_{10}O_{40}$. Here, the slopes in the van't Hoff plots were 0.92 ($r^2 = 0.99$) and 0.91 ($r^2 = 0.99$) for anthracene and xanthene, respectively. Finally, van't Hoff plots for the effect of oxygen pressure yield slopes of 0.001 and 0.068 for

(40) Sullivan, P. D.; Menger, E. M.; Reddoch, A. H.; Paskovich, D. H. *J. Phys. Chem.* **1978**, *82*, 1158.
(41) Eloranta, J.; Sippula, A. *Finn. Chem. Lett.* **1975**, 170.
(42) Dradi, E.; Gatti, G. *J. Am. Chem. Soc.* **1975**, *97*, 5472.
(43) Nicholas, A. M. P.; Arnold, D. R. *Can. J. Chem.* **1982**, *60*, 2165.

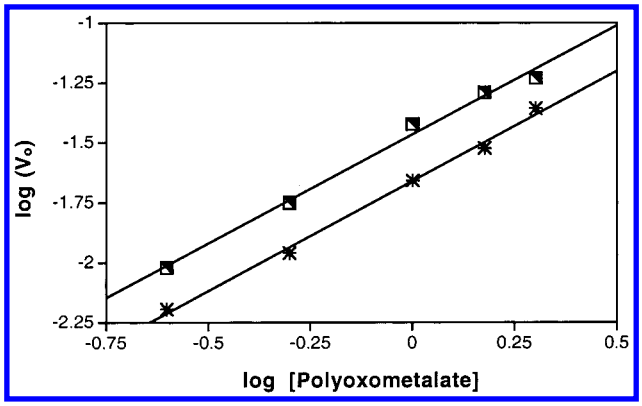

Figure 9. Rate of reaction as a function of $H_5PV_2Mo_{10}O_{40}$ concentration. Reaction conditions: 9 mM substrate and 0.25−2.0 mM $H_5PV_2Mo_{10}O_{40}$ in 2 mL of acetonitrile, 1 atm O_2, 60 °C. Asterisk (*), anthracene; ◥, xanthene.

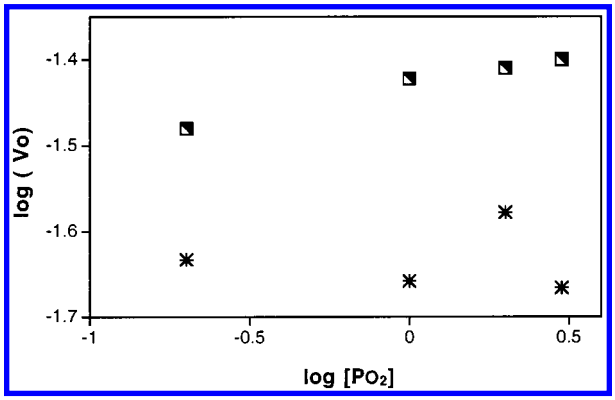

Figure 10. Rate of reaction as a function of the oxygen pressure. Reaction conditions: 9 mM substrate and 1.0 mM $H_5PV_2Mo_{10}O_{40}$ in 2 mL of acetonitrile, 0.2−3 atm O_2, 60 °C. Asterisk (*), anthracene; ◥, xanthene.

anthrancene and xanthene, respectively. Statistical T-test analysis on the slopes showed that these values are, in effect, zero at greater than 99% confidence limits. Thus, the reactions can be concluded to be zero-order in molecular oxygen. These results clearly allow the conclusion that the rate-determining step is during the hydrocarbon oxidation by the $H_5PV_2Mo_{10}O_{40}$ and not during the oxidative regeneration of the catalyst, Scheme 1. Notable also in this context is the observation that under anaerobic and stoichiometric conditions, the rate of formation of anthraquinone and xanthen-9-one is the same, within 5%, as it is under catalytic aerobic conditions. Subsequent reoxidation of the reduced catalyst is very fast (see also previous research in this area[19k]). Reactions as a function of temperature and the relevant Eyring or Arrhenius plots yielded the following complete empirical rate equations for the oxidation of anthracene (eq 4) and xanthene (eqn 5).

$$\frac{-\mathrm{d[RH]}}{\mathrm{d}t} = k_{\mathrm{obs}}[\mathrm{RH}]^1[\mathrm{POM}]^1[\mathrm{O_2}]^0$$
$$\Delta H^{\ddagger} = 19.0 \text{ kcal/mol}, \Delta S^{\ddagger} = -54 \text{ cal/mol/K} \quad (4)$$

$$\frac{-\mathrm{d[RH]}}{\mathrm{d}t} = k_{\mathrm{obs}}[\mathrm{RH}]^1[\mathrm{POM}]^1[\mathrm{O_2}]^0$$
$$\Delta H^{\ddagger} = 7.5 \text{ kcal/mol}, \Delta S^{\ddagger} = -46 \text{ cal/mol/K} \quad (5)$$

Having determined that the rate-determining step was during the hydrocarbon oxygenation rather than the oxidative regeneration of the catalyst, we sought to look at deuterium isotope effects. First, in a competitive reaction between anthracene (10 mM), anthracene-d_{10} (10 mM), and $H_5PV_2Mo_{10}O_{40}$ (1 mM) in CH_3CN at 60 °C and 1 atm O_2, an inverse kinetic isotope effect, $k_H/k_D = 0.85 \pm 0.05$, for the formation of anthraquinone was measured. This result is consistent with a change of hybridization from sp^2 to sp^3 at the 9(10) aromatic carbon of anthracene in the rate-determining step.[44] Therefore, in the rate-determining step, there must be formation of a C−O bond at the 9(10) aromatic carbon of anthracene. Similarly, the kinetic isotope effect was measured for xanthene/xanthene-9-d_2 (20 mM) and $H_5PV_2Mo_{10}O_{40}$ (1 mM) in CH_3CN at 60 °C and 1 atm O_2. A kinetic isotope effect, $k_H/k_D = 2.3 \pm 0.1$, for the formation of xanthen-9-one was obtained. This result, combined with the observation of the xanthenyl cation in the ^{1}H NMR spectrum upon reaction of xanthene and $H_5PV_2Mo_{10}O_{40}$ under anaerobic conditions, and the identical isotope effect in the electron transfer between xanthene and $H_5PV_2Mo_{10}O_{40}$, leads to the conclusion that the rate-determining step in this case is the formation of a xanthenyl cation.

Reoxidation of the Reduced Polyoxometalate. According to the Mars−van Krevelen mechanism (Scheme 1), the original catalyst is regenerated by reaction of the reduced and deoxygenated polyoxometalate and protons with molecular oxygen with coformation of water. In the present case, the study of the reoxidation step is complicated by two factors. First, from a kinetic point of view, the reoxidation is not rate-determining and is also very fast.[19k] Second, there are fast exchange reactions between the oxygen atom in water and the terminal and bridging oxygen atoms in $H_5PV_2Mo_{10}O_{40}$, as mentioned above and noted in the literature.[45] Taking this into account, two diametrical scenarios can be pictured for the polyoxometalate regeneration. In the first scenario, the deoxygenated polyoxometalate reacts first with water to yield a reoxygenated, but still reduced, polyoxometalate. The latter is then reoxidized by molecular oxygen, and water is then formed again. Alternatively, as is accepted for the Mars−van Krevelen mechanism in the gas phase, the polyoxometalate framework oxygen atoms are replaced directly by molecular oxygen with coformation of water. A manifestation of these opposing views can also be inferred from some reports described in the literature. Kawafune was the first to study the reaction between triphenylphosphine and $PMo_{12}O_{40}^{3-}$ and claimed that an oxygen transfer was taking place and claimed observation and isolation of the deoxygenated $[PMo_{12}O_{40-z}]^{q-}$ ($z = 1, 2, 3$) species.[46] Just recently,[47] the oxygen-transfer reaction mechanism has been challenged, and the identification of $[PMo_{12}O_{39}]^{3-}$ has been disputed and revised to $[HPMo_{12}O_{40}]^{4-}$ [45b] or $[H_2PMo_{12}O_{40}]^{3-}$.[45a] Unfortunately, in none of the reports has isotope labeling been used. Rather, the supposed polyoxometalate species have been inferred from changes in the ^{31}P NMR and IR spectra and different electrochemical properties of the various species. It should also be pointed out that oxygen transfer from various organic substrates, for example, sulfoxides to oxygen-deficient polyoxometalates, has been demonstrated.[48]

For the oxidation of hydrocarbons, the presence of vanadium in the polyoxometalate was obligatory; thus, $H_5PV_2Mo_{10}O_{40}$ was more reactive than $H_4PVMo_{11}O_{40}$, and $H_3PMo_{10}O_{40}$ showed no

(44) Streitwieser, A., Jr.; Jagow, R. H.; Fahey, R. C.; Suzuki, S. *J. Am. Chem. Soc.* **1958**, *80*, 2326.
(45) Duncan, D. C.; Hill, C. L. *J. Am. Chem. Soc.* **1997**, *119*, 243.
(46) (a) Kawafune, I. *Chem. Lett.* **1986**, 1503. (b) Kawafune, I.; Matsubayashi, G. *Chem. Lett.* **1992**, 1869. (c) Kawafune, I.; Matsubayashi, G. E. *Inorg Chim. Acta* **1991**, *188*, 33. (d) Kawafune, I.; Matsubayashi, G. E. *Bull. Chem. Soc. Jpn.* **1994**, *67*, 694.
(47) (a) Artero, V.; Proust, A. *Eur. J. Inorg. Chem.* **2000**, 2393. (b) Neier, R.; Trajanovski, C.; Mattes, R. *J. Chem. Soc., Dalton Trans.* **1995**, 2521.
(48) Piepgrass, K.; Pope, M. T. *J. Am. Chem. Soc.* **1989**, *111*, 753.

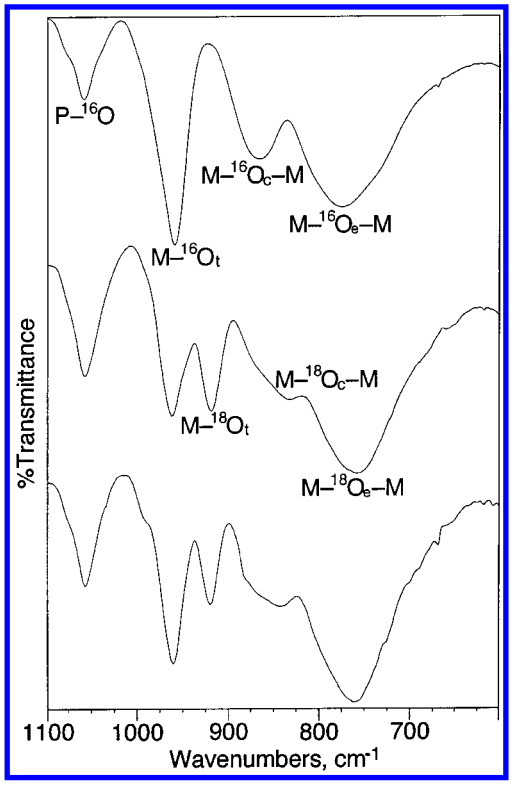

Figure 11. IR spectra of ^{18}O-labeled $H_5PV_2Mo_{10}O_{40}$ before and after reaction with anthracene and $^{16}O_2$. Top, $H_5PV_2Mo_{10}{}^{16}O_{40}$; middle, $H_5PV_2Mo_{10}{}^{18}O_{40}$ with 50% ^{18}O at the terminal positions and 90% ^{18}O at the corner and edge positions; bottom, spectrum after reaction with anthracene and $^{16}O_2$ (10 mM $H_5PV_2Mo_{10}{}^{18}O_{40}$ and 60 mM anthracene in 1 mL of dry acteonitrile, 1 atm $^{16}O_2$).

catalytic activity. Under anaerobic conditions in reactions carried out with $H_5PV_2Mo_{10}O\cdot 34H_2O$ as catalyst in CD_3CN, the ^{31}P NMR showed no formation of new peaks, but others disappeared or slightly shifted because of the effect of the paramagnetic V^{IV} centers.[19k] The polyoxometalate reoxidation step was also investigated by measurement of the IR spectra of ^{18}O-enriched $H_5PV_2Mo_{10}O_{40}$ after catalytic reaction with anthracene under $^{16}O_2$ (Figure 11). The peaks for terminal, corner-, and edge-shared oxygen atoms in $H_5PV_2Mo_{10}{}^{18}O_{40}$ at 919, 831, and 758 cm^{-1} are shifted relative to peaks in unlabeled $H_5PV_2Mo_{10}{}^{16}O_{40}$ at 960, 865, and 774 cm^{-1}. After aerobic ($^{16}O_2$) oxidation of anthracene (60 mM anthracene, 1 mM $H_5PV_2Mo_{10}{}^{18}O_{40}$ (75% ^{18}O) in CH_3CN, 60 °C, 1 atm $^{16}O_2$), a 69% incorporation of ^{18}O into anthraquinone was observed, along with an increase in the peak ratio of 960 (^{16}O) vs 919 cm^{-1} (^{18}O). Shifts from 831 to 843 cm^{-1} and 758 to 761 cm^{-1} were observed for the corner- and edge-shared positions, respectively. Clearly, there appears to be direct or indirect reincorporation of ^{16}O from $^{16}O_2$ into the polyoxometalate.

^{17}O-enriched $H_5PV_2Mo_{10}O_{40}$ was also prepared by treating 10 μmol of dehydrated $H_5PV_2Mo_{10}{}^{16}O_{40}$ with 500 μmol of $H_2{}^{17}O$ (10.2% ^{17}O) in 1 mL of dry acetonitrile for 6 days to obtain an equilibrated system. The ^{17}O NMR of the solution obtained (Figure 12 bottom) shows the incorporation of ^{17}O in the terminal, V═O (1290 ppm), and Mo═O (935 ppm) positions, and in the bridging Mo−O−Mo, Mo−O−V, and V−O−V positions (540−590 ppm). After addition of 100 μmol of anthracene and reaction under $^{16}O_2$ (55% conversion), two major changes in the ^{17}O NMR spectrum (Figure 12, top) are observed. First is the appearance of a peak at 515 ppm assigned to [^{17}O]anthraquinone.[49] Second is the different "fingerprint" associated with the peaks for oxygen in the bridging positions.

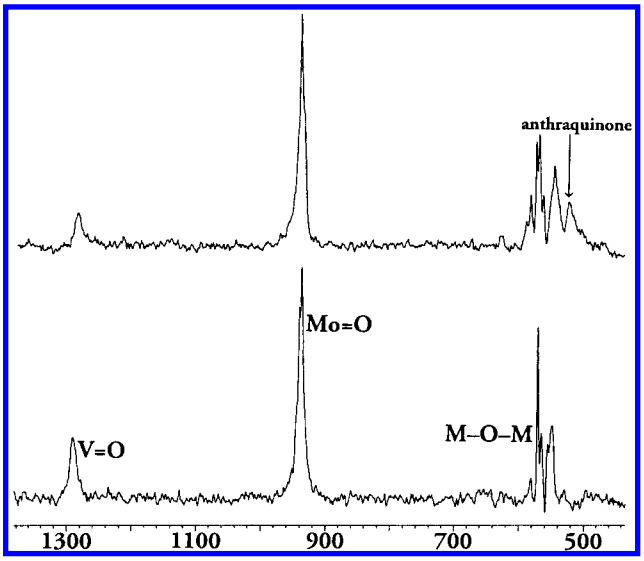

Figure 12. ^{17}O NMR spectra of ^{17}O-labeled $H_5PV_2Mo_{10}O_{40}$ before (bottom) and after (top) reaction with anthracene and $^{16}O_2$.

There is also a less significant decrease in the relative intensity of the peak associated with V = ^{17}O. Again, it is difficult to draw an exact conclusion from the changes in the ^{17}O NMR. However, with some degree of confidence, one can say that deoxygenation of the polyoxometalate in the hydrocarbon oxidation step followed by reoxygenation by $^{16}O_2$ and "scrambling" by excess enriched $H_2{}^{17}O$ or vice versa leads to a different distribution of ^{17}O in the polyoxometalate. This would mean that the oxygen transfer from the originally enriched polyoxometalate is site-specific. Since the presence of vanadium is necessary, one may conclude that most likely, oxygen transfer is from positions adjacent to vanadium in the polyoxometalate. Despite these experiments, it is at this point still impossible to resolve the conflicting scenarios mentioned above for polyoxometalate reoxidation.

Summary and Comments on the Reaction Mechanism. A mechanistic scheme for the oxidation of anthracene is given is Scheme 8. The reaction begins with an electron transfer from anthracene to the polyoxometalate. The electron transfer appears to be outer sphere with preassociation between the polyoxometalate and hydrocarbon. From the ESR spectrum of the radical cation-reduced polyoxometalate, one may deduce that a stable donor acceptor complex is formed. Next, there is oxygen transfer from the polyoxometalate to the initially formed radical cation. There is extensive evidence that the source of oxygen in the product is neither from molecular oxygen nor from water. The rate-determining step appears to involve a change in hybridization at the 9(10) carbon from sp^2 to sp^3. In other words, as indicated, the oxygen-transfer step is also rate-determining. Recalling that anthraquinone was the only observed reaction product, the following reaction step(s) is faster; thus, we can at this point only postulate on possible routes to the formation of anthraquinone. First, it is possible that anthraquinone is formed directly from the observed intermediate. Second, it is possible that initially, the first oxidation step yields 9-hydroxyanthracene or the tautomeric anthrone, which is then oxidized very fast to anthraquinone. In separate experiments, the oxidation of anthrone, even at room temperature, is complete in a few seconds.

The oxidation of xanthene occurs by a slightly different pathway (Scheme 9). As with anthracene, the reaction begins

(49) Boykin, D. W.; Baumstark, A. G. *Tetrahedron* **1989**, *45*, 3615.

Scheme 8

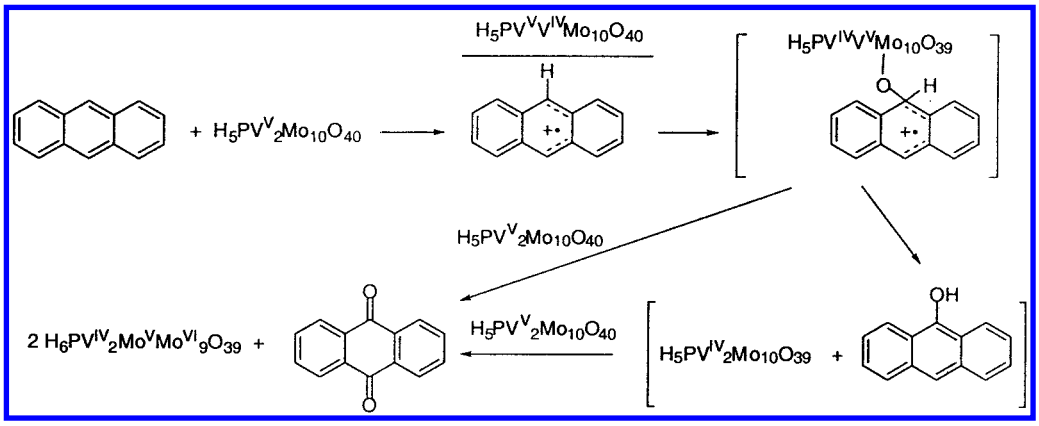

Scheme 9

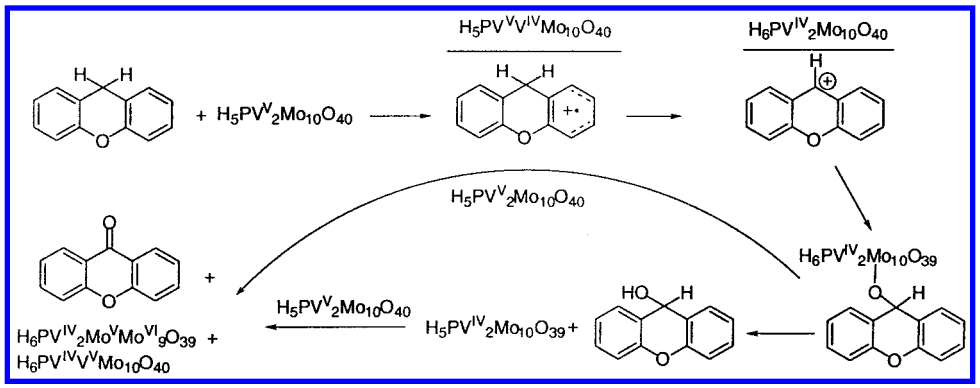

Scheme 10

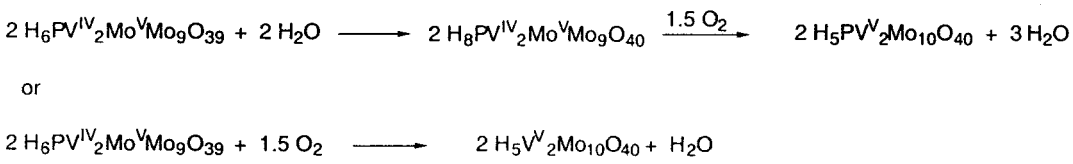

with an electron transfer from xanthene to the polyoxometalate. However, here the radical cation is not observed; rather, as deduced from the ^{1}H NMR spectrum, a stable and observable benzylic cation is formed via additional proton and electron transfer. The kinetics experiments, coupled with the kinetic isotope effect, indicate that the formation of the xanthenyl cation is rate-determining. As in the case of anthracene, there is a wide body of evidence that indicates that there is direct oxygen transfer from the polyoxometalate to the activated xanthene, rather than reaction with molecular oxygen or water. Xanthen-9-ol is not observed, an indication that if formed, it is also very quickly oxidized, presumably by another molecule of polyoxometalate. Alternatively, in the presence of additional catalyst, xanthen-9-one may be formed directly.

The regeneration of the original oxidized form of the catalyst by reaction with molecular oxygen occurs very fast. Thus, we do not have, at this time, any real information concerning this process, because both ^{31}P NMR and IR measurements show the presence of complete Keggin structures formed by the reaction of the proposed oxygen-deficient Keggin species with either water or molecular oxygen, as summarized in Scheme 10.

Finally, a few words should be presented on the scope of the oxygen-transfer reaction described herein. In this manuscript, we have concentrated on understanding the mechanism of the reaction for oxidation of both aromatic and alkyl aromatic compounds. We are presently engaged in developing this catalytic oxidation for synthetic applications, which will be described and published separately.

Experimental Section

Instruments. ^{1}H NMR (250 MHz) and ^{31}P NMR (101.27 MHz, 85% H_3PO_4 external standard) measurements were taken on a Bruker Avance 250 DPX instrument, and ^{17}O NMR (54.25 MHz, $H_2$17O internal standard) measurements were taken on a Bruker Avance 400 instrument.

HPLC analyses were performed on a Merck-Hitachi L6200 equipped with a L4000 UV detector. The column used was a reverse-phase Lichospher 100 RP-18 (5 μm) 25 × 4 mm column using 80% methanol/20% water as eluent at a flow rate of 0.8 mL/min with detection at 242 nm. Retention times: anthracene, 18.1 min; anthraquinone, 9.6 min; xanthene, 16.2 min; xanthen-9-one, 11.7 min.

GC/MS measurements were carried out on an instrument consisting of a HP 5973 mass-selective detector and a HP 6890 GC. A 5% phenyl methylsilicone 0.32 mm i.d., 0.25-μm coating, 30-m-length column (Restek 5MS). The eluent gas was helium.

IR measurements were carried out on a Nicolet Protege 460 FTIR instrument. Solutions of polyoxometalate samples were placed on KBr disks, and the solvent was allowed to evaporate. UV−vis spectra and kinetic experiments were carried out on a HP 8452A diode array UV−vis spectrometer equipped with a stirring apparatus and temperature bath (± 0.1 °C). Cyclic voltammetry was carried out on a BAS-1 instrument. The ESR spectra were recorded on a Bruker ER200D-SRC spectrometer (X-band).

Materials. The $H_5PV_2Mo_{10}O_{40}\cdot 34H_2O$ polyoxometalate was prepared using a known literature method.[50] Thermogravimetric analysis (Mettler 50) indicated 34 water molecules per polyoxometalate. Anal. found (calculated): P, 1.31 (1.34); V, 4.38 (4.41); Mo, 41.32 (41.56). IR: 1057, 960, 865, 774 cm^{-1}. ^{31}P NMR (CD_3COCD_3, 85% H_3PO_4 external standard): −3.96 (6), −3.42 (1), −3.37 (4), −3.31(2), −3.22(2) ppm (area of peak). $Q_5PV_2Mo_{10}O_{40}$ ($Q = (C_4H_9)_4N$) was prepared by mixing 10 equiv of QBr dissolved in water to $H_5PV_2Mo_{10}O_{40}$ also dissolved in water. The precipitate formed was filtered and dried overnight in a vacuum oven at 80 °C. The thermogravimetric analysis showed no water was present. Anal. found (calculated): C, 32.09 (32.64); H, 5.99 (6.16); N, 2.13 (2.38). Solvents and substrates available from commercial sources were of the highest purity available and were used without further purification. $^{18}O_2$ (Enritech) was 96.1% ^{18}O-labeled. $H_2{}^{18}O$ (Rotem) was 94.3% ^{18}O-labeled. $H_2{}^{17}O$ (D-Chem) was 10.2% ^{17}O-labeled. Dry acetonitrile (Biolab) contained < 20 ppm water.

Xanthene-9-d_2. Xanthene-9-d_2 was prepared by reduction of xanthen-9-one with $AlCl_3-LiAlD_4$. ^1H NMR and GC/MS was used to verify the absence of benzylic hydrogen atoms and the presence of deuterium.

4-Alkyl Anisole. 4-Ethyl-, 4-*n*-propyl-, and 4-*i*-propylanisole were prepared by reacting 0.1 mol 4-ethyl-, 4-*n*-propyl-, and 4-*i*-propylphenol with 0.12 mol methyliodide and 0.12 mol potassium carbonate (anhydrous) in 100 mL acetone at reflux for 24 h. After filtration, the acetone solvent and excess methyliodide was removed by evaporation; the product was purified over a silica gel column by elution with chloroform ($R_f = 0.90$).

2-Chloroanthracene. A mixture of 2-chloroanthraquinone (4.95 g, 0.02 mol), zinc powder (33 g), 1,4-dioxane (165 mL), and 28% NH_4OH (165 mL) were mixed under reflux for 3 h. The mixture was carefully poured into 500 mL of water and extracted twice with 25 mL of 1,2-dichloroethane. After removal of the 1,2-dichloroethane by vacuum evaporation, the crude product was twice recrystallized from ethanol to yield 1 g (23%) of a yellowish product (>99% purity by GC/MS). mp, 218−219 °C. Anal. found (calculated): C, 78.22 (79.06); H, 4.48 (4.23); Cl, 16.65 (16.70). ^1H NMR ($CDCl_3$): 8.56 (d, 2H), 8.11 (m, 4H), 7.54 (m, 2H), 7.45 (dd, 1H).

2-Methoxyanthracene. 2-chloroanthraquinone (10.52 g, 0.043 mol) was dissolved in a solution derived from 10 g of sodium metal in 100 mL methanol that was heated under reflux for 72 h. The solvent was removed by distillation; water was added, and the mixture was neutralized with dilute H_2SO_4. The solid 2-methoxyanthraquinone was collected and crystallized from ethanol. Yield, 6.1 g, 59%. 2-methoxyanthraquinone (6.0 g, 0.025 mol), zinc powder (40 g), 1,4-dioxane (200 mL), and 28% NH_4OH (200 mL) were mixed under reflux for 3 h. The yield was 0.5 g (10%) with a purity of >98% by GC/MS after treatment as described above. mp, 182−183 °C. Anal. found (calculated): C, 86.93 (86.54); H, 5.89 (5.77). ^1H NMR ($CDCl_3$): 8.35 (s, 1H), 8.27 (s, 1H), 7.93 (m, 2H), 7.89 (d, 1H), 7.40 (m, 2H), 7.20 (d, 1H), 7.16 p(dd, 1H), 3.92 (s, 3H).

$H_5PV_2Mo_{10}{}^{18}O_{40}$. ^{18}O-labeled $H_5PV_2Mo_{10}O_{40}$ was prepared by drying the polyoxometalate at 120 °C for 24 h and then adding 50 equiv $H_2{}^{18}O$ (94.3%) in dry CH_3CN and mixing for 18 h. The drying-exchange cycle was repeated 3 times. ^{18}O enrichment was estimated to be ∼50% at the terminal oxygen atoms and >90% at the edge- and corner-shared oxygen atoms. The enrichment and the bridging oxygen atoms were estimated by deconvolution of the IR spectra assuming a theoretical 40 cm^{-1} isotope shift and expected equal peak intensities for labeled and unlabeled oxygen. Total enrichment for potentially transferable oxygen atoms, that is, excluding the four internal oxygen atoms, was therefore ∼75%.

$H_5PV_2Mo_{10}17O_{40}$. ^{17}O-labeled $H_5PV_2Mo_{10}O_{40}$ was prepared by drying the polyoxometalate at 120 °C for 24 h and then adding 50 equiv $H_2{}^{18}O$ (10.2%) in dry CH_3CN and mixing for 6 days in order to obtain a fully equilibrated compound.

Oxidation Reactions. Reactions under aerobic conditions were carried out using 25-mL Ace glass pressure tubes. The tubes were charged with the appropriate amounts of substrate, catalyst, and solvent and were gently flushed with oxygen for 5 min. For experiments with $^{18}O_2$, two freeze−pump−thaw cycles instead of flushing were used to fill the reaction tube. The pressure was brought to 1 atm, and the reactions were initiated by placing the reaction vessel in a thermostated oil bath, usually at 60 ± 0.5 °C. At the desired time interval, 10-μL aliquots were removed for HPLC analysis, or 1-μL aliquots were removed for GC-MS analysis. In kinetic experiments, the reaction tube was immediately repressurized. In general, HPLC was used for kinetics experiments and determination of product yields. The sample aliquots for HPLC analysis were diluted in the eluent, and for GC/MS analysis, the aliquots were directly injected. ^{18}O incorporation was measured from the mass spectra by comparing peak intensities. For experiments using anthracene, anthraquinone product peaks at $m/z = 208$, 210, and 222 were compared. For xanthene, xanthen-9-one intensities of peaks at $m/z = 196$ and 198 were compared. For water peaks (retention time, 1.12 min) at $m/z = 18$ and 20 were compared. Reactions under anaerobic conditions were carried out either in 25-mL Ace glass pressure tubes or directly in 5-mm NMR tubes equipped with a vacuum/pressure valve. The tubes were charged with the appropriate amounts of substrate, catalyst, and solvent and were gently flushed with argon for 5 min. The tubes were then frozen, pumped down, filled with argon, and then thawed. This procedure was repeated three times until final pressurization to 1 atm argon. HPLC analysis was done as described above, and ^1H NMR spectra were measured directly. Oxygen uptake was measured by use of a gas buret. Kinetic isotope effect for oxidation of anthracene/anthracene-d_{10} was measured in a competitive reaction by reacting anthracene (10 mM), anthracene-d_{10} (10 mM), and $H_5PV_2Mo_{10}O_{40}\cdot 34H_2O$ (1 mM) in acetonitrile at 60 °C and 1 atm O_2. Peaks were quantified by comparing molecular peak intensities of anthraquinone and anthraquinone-d_8. The kinetic isotope effect for oxidation of xanthene was studied by the comparison of reaction rates of xanthene and xanthen-9-d_2 oxidized separately. Thus, xanthene or xanthen-9-d_2 (20 mM) and $H_5PV_2Mo_{10}O_{40}\cdot 34H_2O$ (1 mM) in acetonitrile at 60 °C and 1 atm O_2 were reacted, and the rate of xanthen-9-one formation was measured by HPLC using benzoic acid as calibration standard.

Kinetic Profiles of Interaction of Hydrocarbons with $H_5PV_2Mo_{10}O_{40}$. A solution of 1 μmol of $H_5PV_2Mo_{10}O_{40}$ in 3 mL of acetonitrile was purged with argon for 20 min in a quartz cuvette and then brought to 60 °C. The reaction was initiated by the injection via GC syringe of 20 μmol of hydrocarbon, and the reduction of the polyoxometalate was followed at 750 nm in the UV−vis spectrometer. First-order rate constants ($r^2 = 0.99$) were computed from the data.

Cyclic Voltammetry. The electrochemical potentials of xanthene and xanthen-9-d_2 were measured using a glass carbon cathode, a platinum anode and calomel reference electrode. The measurements were of solutions of 10 mM substrate in 100 mM tetrabutylammonium tetrafluorborate in dichloromethane at 50 mV/sec; I/V = 500 μA/V.

Electron Spin Resonance. Spectra were measured by preparing solutions of 2 mM anthracene or xanthene and 4 mM $Q_5PV_2Mo_{10}O_{40}$ in 1,1,1,3,3,3-hexafluoro-2-propanol or 4 mM $H_5PV_2Mo_{10}O_{40}$ in acetonitrile under argon and heating at 40 °C for the indicated time period in a quartz capillary tube (1 mm, 200 μL). Spectra were recording using microwave frequency, 9.78 GHz; microwave power, 12 mW; field modulation, 320mG; receiver gain, 4×10^5; time constant, 320 ms; and scan time, 200 s. The Public EPR Software Tools developed by D. Duling (NIEHS/NIH) were used for the computer simulation.

Acknowledgment. This research was supported by the Basic Research Foundation administered by the Israeli Academy of Science and Humanities.

JA004163Z

(50) Tsigdinos, G. A.; Hallada, C. J. *Inorg. Chem.* **1968**, *7*, 437.
(51) Parker, V. D. *J. Am. Chem. Soc.* **1976**, *98*, 98.
(52) Zhang, X.; Bordwell, F. G. *J. Org. Chem.* **1992**, *57*, 4163.
(53) Freccero, M.; Pratt, A.; Albini, A. Gong, C. *J. Am. Chem. Soc.* **1998**, *120*, 284.